Modelling of the pulsed field magnetization of a (RE)BaCuO bulk with a superconducting weld

Rémi Dorget, Kévin Berger, Longji Dadiel, Kimiaki Sudo, Naomichi Sakai, Tetsuo Oka, Masato Murakami, Jean Lévêque

Modelling of the pulsed field magnetisation of a REBaCuO bulk with a superconducting weld

R Dorget[1,2], K Berger[1], J Longji Dadiel[3], K Sudo [3], N Sakai[3], T Oka[3], M Murakami[3], J Lévêque[1]

[1]Université de Lorraine, GREEN, F-54000 Nancy, France
[2]Safran Tech, Electrical & Electronic Systems Research group, Rue des Jeunes Bois, Châteaufort, 78114 Magny-Les-Hameaux, France
[3]Shibaura Institute of Technology ,3 Chome-7-5 Toyosu, Koto, Tokyo 135-8548 - Japan

*remi.dorget@univ-lorraine.fr

Abstract. The Pulsed Field Magnetization (PFM) is a compact and fast method to magnetize superconducting bulks compared to quasi-static magnetization methods like field- or zero-field-cooling. However, the heat generation induced by the strong applied variable magnetic field during the PFM makes high trapped magnetic field harder to achieve. In order to make the REBaCuO bulks easier to magnetize by PFM, superconducting bulks including a superconducting weld are studied by considering the electromagnetic properties of the weld different from those of the bulk body. This artificial grain boundary obtained by superconducting welding method might increase the trapped magnetic flux without increasing the applied magnetic field. In this paper, we are modelling the superconducting weld behavior during PFM using a 3D finite element model with the software COMSOL Multiphysics. The simulations are based on an H-formulation from Maxwell's equations and the heat diffusion equation. We analyse the impact of the critical current J_c of the weld on the trapped magnetic field.

1. Introduction

The superconducting welding process for REBaCuO bulks consist of the use of a superconducting solder material with a low peritectic temperature to make an artificial grain boundary between two single grain bulks. The solder material for YBaCuO can be a REBaCuO with an heavy rare earth such as YbBaCuO or ErBaCuO [1–6] or YBaCuO with a dopant reducing its melting point such as Ag or Ag_2O [7–11]. The superconducting process is similar to the multi seeded melt growth technique (MSMG) as the two welded bulks acts as the seeds giving their crystal orientation to the weld material. This process and its crystallization is well known in the literature [12] and it has been shown that the grain connection of superconducting welds is better than MSMG [13]. However, the magnetization of bulks obtained by the welding process has only been studied in field cooling at 77 K.

The pulsed field magnetization (PFM) appears to be a more compact way to magnetize superconducting bulk compared to quasi-static magnetization methods like field- or zero-field-cooling. However, the applied magnetic field during PFM must be very large for the flux to reach the sample centre and completely magnetize the bulk. Consequently, the heat generation induced by fast flux motion during the pulse decrease the maximum achievable trapped field [14]. In order to increase the

trapped flux obtained by PFM, a superconducting weld placed at the middle of the bulk is considered with a critical current J_c weaker than the bulk body. By doing so, we are expecting the magnetic field to penetrate the bulk through the weld, thus reducing the required applied field to fully magnetize the sample.

In this paper, we are simulating by Finite Element Method (FEM) the PFM of a superconducting bulk including a junction with different critical currents on a 3D model implemented on the software COMSOL Multiphysics.

2. Numerical model description

2.1. Simulated setup

Figure 1 shows the PFM setup we are trying to model which consists of a bulk with a superconducting weld placed on the cold head of a cryocooler. These two elements are in a cryostat and surrounded by a magnetizing coil located outside the cryostat.

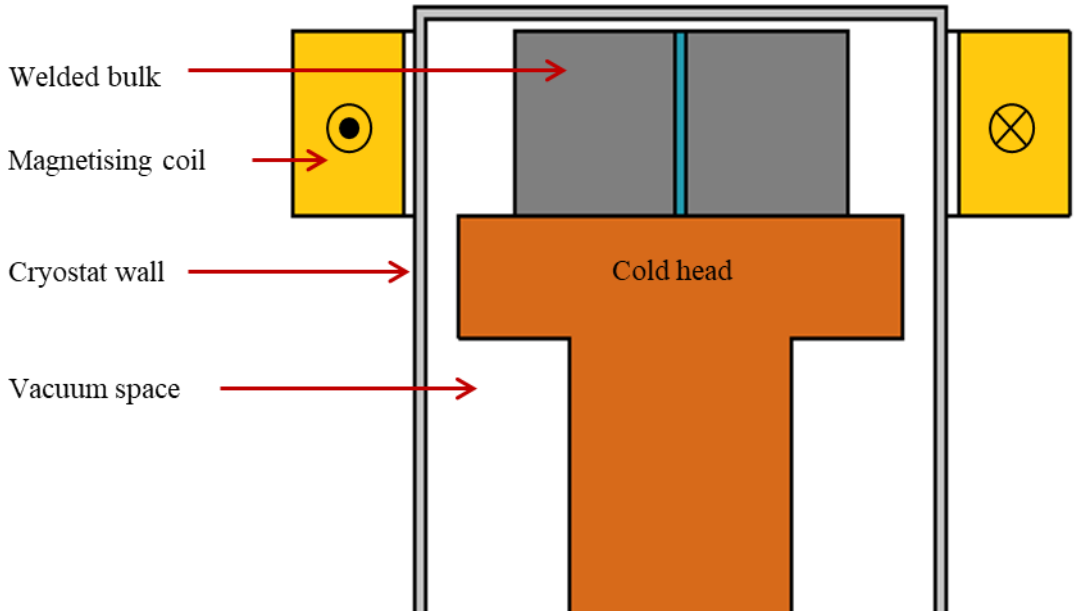

Figure 1. Representation of the main elements in a PFM device

Figure 2 shows the representation of the studied bulk which is 30 mm in diameter and 15 mm in height and comprise a 1 mm thick superconducting weld at the centre.

2.2. Electromagnetic model

The electromagnetic behaviour of the system will be modelled through an ***H***-formulation of the Maxwell equations in 3-D in which the governing equations are the Faraday's and Ampere's laws [14]:

$$\nabla \times \boldsymbol{E} = -\mu_0 \frac{d\boldsymbol{H}}{dt} \quad (1)$$

$$\nabla \times \boldsymbol{H} = \boldsymbol{J} \quad (2)$$

Where $\boldsymbol{H}$ is the magnetic field, $\boldsymbol{E}$ the electric field, $\boldsymbol{J}$ the current density and μ_0 the vacuum magnetic permeability. As implied by equation (1), all materials in the model have a relative permeability equal to 1. In order to simplify the electromagnetic model, the induced currents in the cold head and in the cryostat wall are neglected. Additionally, the magnetising coil is modelled as a homogeneous applied flux density $B_a(t)$ in the **z**-direction perpendicular to the bulk surface with the following expression:

$$B_a(t) = B_{max}\frac{t}{\tau}\exp\left(1-\frac{t}{\tau}\right) \quad (3)$$

where B_{max} is the applied flux density peak value and τ is the time constant of the magnetisation circuit. The applied field is considered in the model as a Dirichlet boundary condition at the external limits of the model geometry.

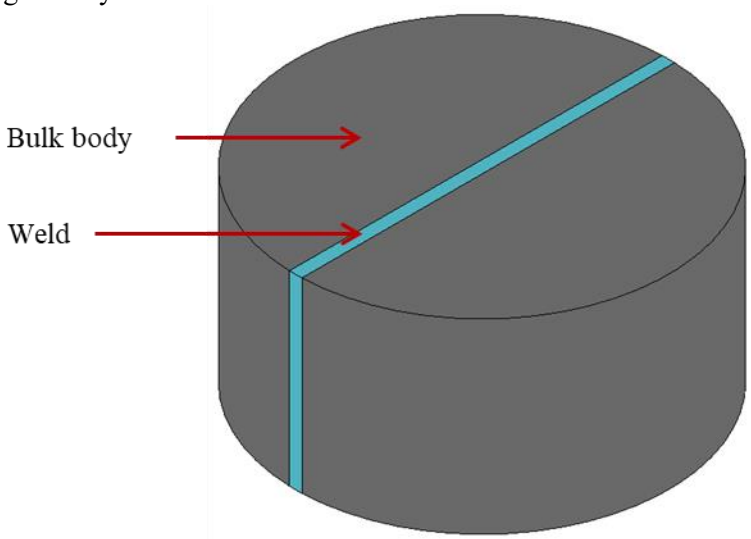

Figure 2. Representation of the bulk comprising a superconducting weld at its centre separating the bulk into two parts.

Thus, the only remaining elements to be simulated are the bulk and the weld which are, in the simulation, surrounded by vacuum. The electromagnetic behaviour of the superconducting parts is modelled though the well-known *E-J* power law where $\boldsymbol{E}$ and $\boldsymbol{J}$ are parallel and linked by the following expression:

$$\|\boldsymbol{E}\|(J,\boldsymbol{B},T) = E_c\left(\frac{\|\boldsymbol{J}\|}{J_c(\boldsymbol{B},T)}\right)^{n(\boldsymbol{B},T)} \quad (4)$$

Where $E_c = 1\ \mu V/cm$ is the critical electric field, $J_c(\boldsymbol{B},T)$ is the critical current density of the material and $n(\boldsymbol{B},T)$ is the exponent of the power law. J_c and n are the superconducting properties of the material and depend on the local flux density and temperature. The dependence of J_c with $\boldsymbol{B}$ is given by the Kim's model [15] and the relation between J_c and the temperature T is assumed to be linear as was done in [16]. Hence, the critical current density of the bulk body $J_{c,b}(\boldsymbol{B},T)$ is expressed as:

$$J_{c,b}(\boldsymbol{B},T) = \frac{J_{c0}}{(1+\|\boldsymbol{B}\|/B_0)^{\beta}} \times \frac{1-T/T_c}{1-T_0/T_c} \quad (5)$$

where J_{c0} is the critical current density for $\|\boldsymbol{B}\| = 0$ and $T = T_0$, B_0 and β are Kim's model constants. T_0 is the reference temperature (77 K) whereas T_c is the critical temperature.

The superconducting weld critical current $J_{c,w}(\boldsymbol{B},T)$ has an expression identical to (5) except for one coefficient α which is equal to the ratio between $J_{c,w}$ to $J_{c,b}$:

$$J_{c,w}(\boldsymbol{B},T) = \alpha\frac{J_{c0}}{(1+\|\boldsymbol{B}\|/B_0)^{\beta}} \times \frac{1-T/T_c}{1-T_0/T_c} \quad (6)$$

Different values of α will be explored to investigate the weld influence. The expression of $n(\boldsymbol{B},T)$ is identical for both the weld and the bulk body:

$$n(\boldsymbol{B},T) = \left(n_1 + \frac{n_0-n_1}{1+\|\boldsymbol{B}\|/B_0}\right)\frac{T_0}{T} \quad (7)$$

where n_0 is the n-exponent of (4) at T_0 and $\|\boldsymbol{B}\| = 0$ whereas n_1 is the n-exponent at $\|\boldsymbol{B}\| \gg 0$. Because of the losses, the temperature may locally exceed the critical temperature. Therefore, the model has to consider a possible transition between superconducting and normal state. For this purpose, we define two resistivity, the normal state resistivity ρ_n, which is assumed constant, and the superconducting resistivity ρ_s derived from (4). The transition between both resistivity is modelled using transition functions. The resulting expression of the material resistivity ρ is:

$$\rho = \frac{1 - \tanh\left(\frac{T_c - T}{0.2}\right)}{2} \times \rho_s(J, \boldsymbol{B}, T) + \frac{1 - \tanh\left(\frac{T - T_c}{0.2}\right)}{2} \times \rho_n \tag{8}$$

2.3. Thermal model

The thermal model computing the temperature distribution over time is solving the heat diffusion equation:

$$\gamma C \frac{dT}{dt} - \nabla \cdot (\kappa \nabla T) = Q \tag{9}$$

where γ is the density, C the specific heat and κ the thermal conductivity. Because of the movement of the magnetic flux, the superconductor is generating heat during the magnetisation. The heat per volume unit Q is coupled to the electromagnetic model by:

$$Q = \boldsymbol{E} \cdot \boldsymbol{J} \tag{10}$$

In order to simplify the model, the cryocooler cold head is not directly simulated here. Instead we assume the cold head conductivity to be perfect and that the cryocooling power P_{cryo} is directly available at the bottom surface of the bulk. Thus, only the bulk is considered in the thermal model and the boundary condition at the bulk bottom surface is:

$$\kappa \nabla T \cdot \boldsymbol{n} = \frac{P_{cryo}}{S_{bot}} \tag{11}$$

where $\boldsymbol{n}$ is the vector perpendicular to the surface and S_{bot} is the bottom surface area. The condition applied to the other surfaces corresponding to a perfect thermal insulation is:

$$\nabla T \cdot \boldsymbol{n} = 0 \tag{12}$$

2.4. Symmetries and model parameters

According to the symmetries of the electromagnetic and thermal models, only a quarter of the total bulk geometry need to be simulated. Figure 3 shows the geometry and mesh used for the bulk and its weld.

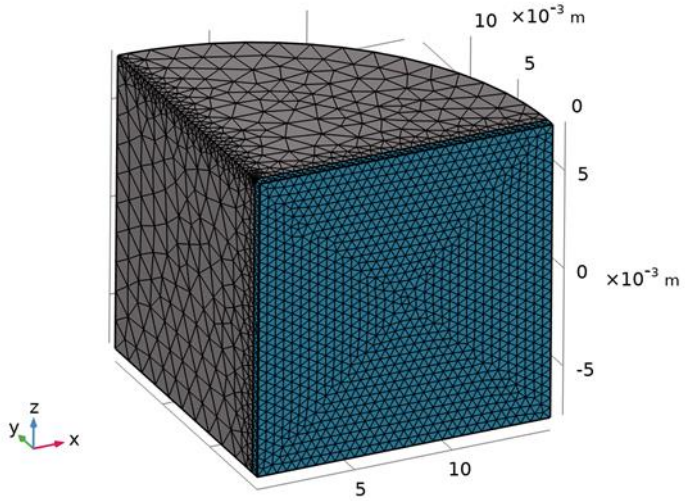

Figure 3. Mesh of the simulated part of the bulk and its weld. The simulated part is ¼ of the complete bulk.

Finally, the values of the parameters are listed in table 2. In the present study, different values of the applied field B_a and the ratio α will be explored to assess the impact of the weld on the trapped field.

Table 1. Simulation parameters

Parameter	Value	Description
J_{c0}	300 A/mm^2	Self-field critical current density at 77 K
B_0	0.5 T	Magnetic field dependence constant
β	1.2	Magnetic field dependence exponent
n_0	20	n-exponent at 77 K and $\|\|\boldsymbol{B}\|\| = 0\ T$
n_1	6	n-exponent at 77 K and $\|\|\boldsymbol{B}\|\| \gg 0\ T$
ρ_n	500 μΩ cm	Normal state resistivity
T_c	92 K	Critical temperature
T_0	77 K	Reference temperature
T_a	60 K	Initial temperature
B_a	[0.5 T : 5 T]	Applied magnetic flux density
τ	10 ms	Pulse time constant
α	[0.25: 1]	Weld to bulk body critical current ratio
P_{cryo}	-50 W	Cooling power of the cryocooler
γ	6 g/cm^3	Density
C	150 J/(kg K)	Heat capacity
κ	5 W/(m K)	Thermal conductivity

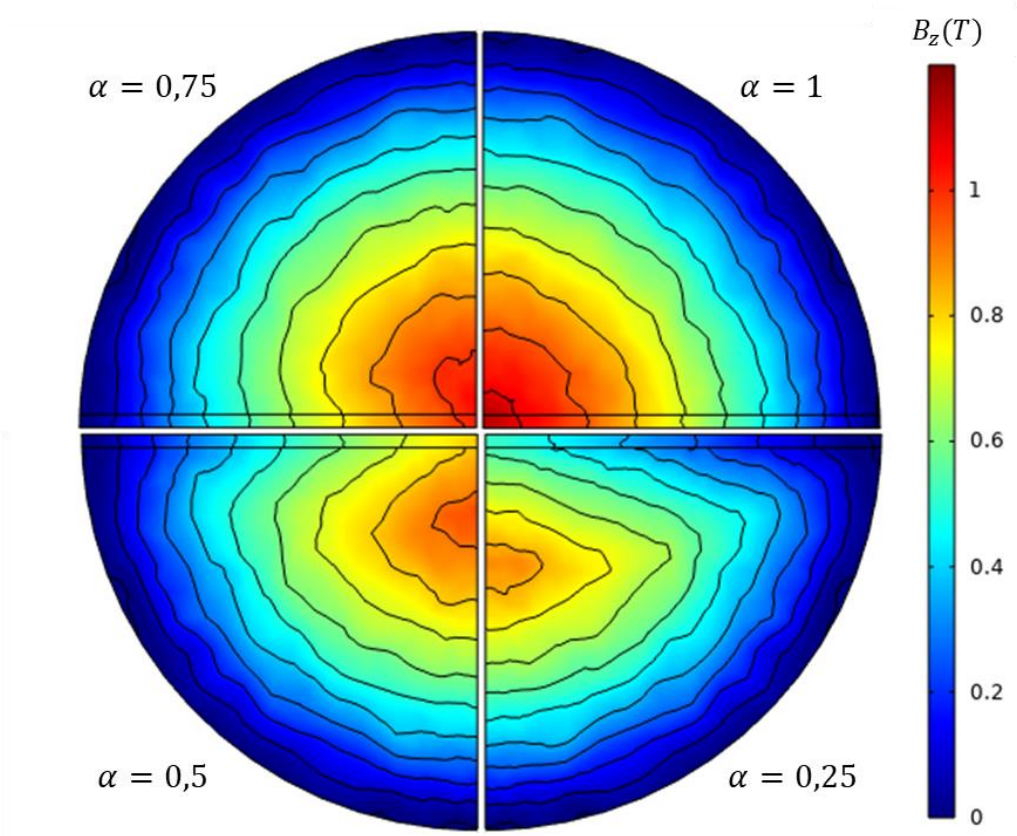

Figure 4. Trapped field map at the bulk surface for different values of α (0.25, 0.5, 0.75 and 1) for an applied field of 4 T.

3. Results

Figure 4 shows the trapped flux density map at the surface of the bulk 60 s after the pulse for different values of α for an applied field of 4 T leading to a complete penetration of all bulks. It should be noted that the value $\alpha = 1$ correspond to the reference case of a normal bulk without weld. We can observe that the peak value of the trapped field is not located at the bulk centre for $\alpha \neq 1$. Indeed, the magnetic flux is penetrating the bulk easily through the weld and is behaving similarly to the bulk edge. Therefore, the peak value is shifted from the centre. Additionally, is appears that the maximum trapped field is decreasing for low J_c welds. Figure 5 shows the maximum value of the flux density at the bulk surface and the applied field during the pulse. We can observe more clearly the decrease in trapped field value on this figure.

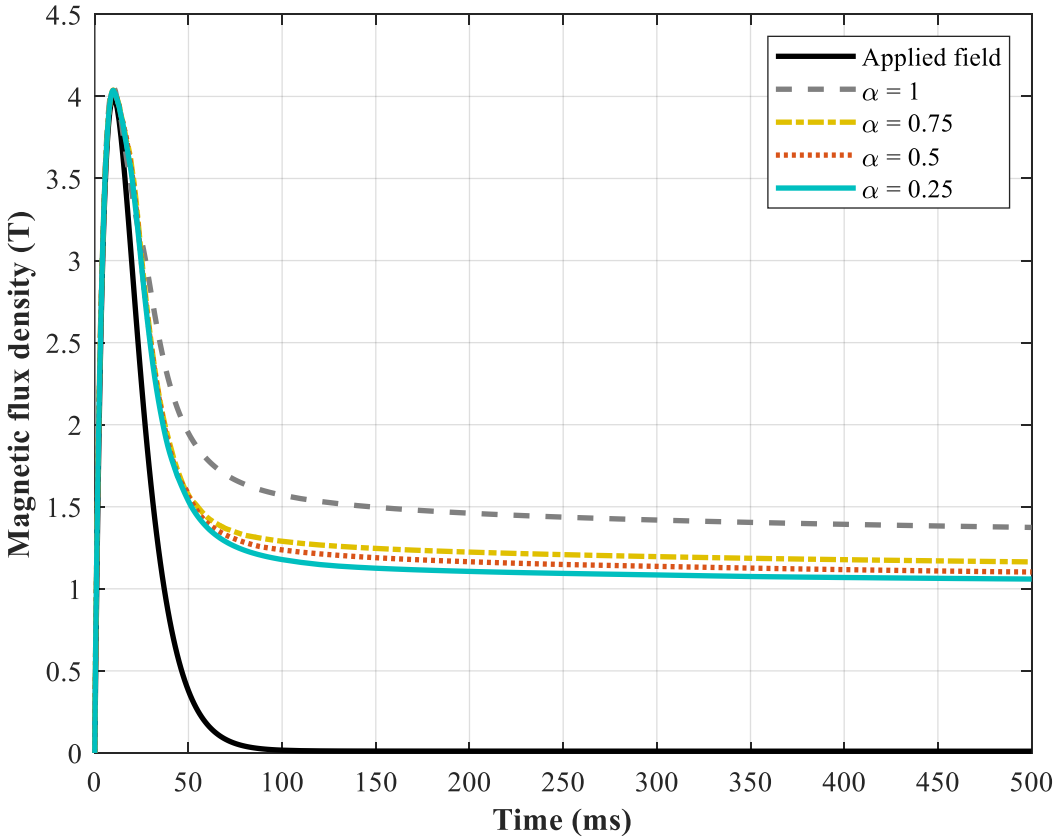

Figure 5. Evolution of the maximum flux density at the bulk surface for different values of α.

In usual magnetic applications such as electrical machines, the trapped flux is more important than the field peak value. Thus, figure 6 shows the trapped flux at the bulk surface for the different values of α function of the applied magnetic field. We can observe two part on this graph. Above 2 T, all bulks are completely penetrated and the trapped flux in the non-welded bulk ($\alpha = 1$) is superior to the welded bulks trapped flux. However, below 2 T, the bulks are not completely penetrated and the ones comprising a low J_c weld have a higher trapped flux (up to 13 % gain). It is interesting to note that for the 2 T pulse, the trapped flux for $\alpha = 1$, $\alpha = 0.25$ and $\alpha = 0.75$ are similar whereas the trapped flux for $\alpha = 0.5$ is larger meaning that there is an optimal value of α at this point which is not 0 nor 1.

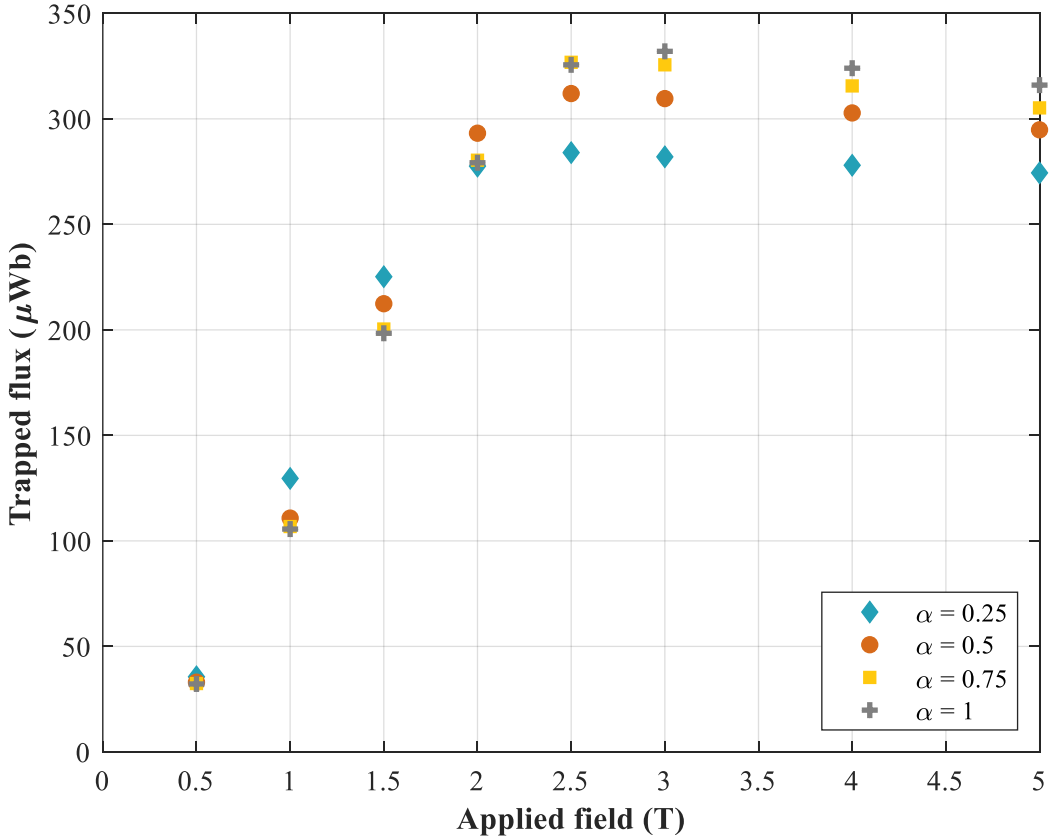

Figure 6. Trapped magnetic flux on the bulk top surface for different values of α function of the applied magnetic flux density.

Since the flux in entering the bulk through the weld, the latter is likely to be subjected to an important amount of losses because of the fast flux motion during the pulse. Indeed, figure 7 shows the average temperature of the weld and the bulk body during a 4 T pulse for $\alpha = 0.5$. It can be clearly seen that the temperature rise in the weld is much more significant than in the bulk body with a difference up to 14 K.

Additionally, two peaks can be observed for the weld average temperature. Indeed, the heat is generated during the rise and the drop of the applied field as the electrical field is created by the derivative of the flux density over time. Therefore, while the field is rising, much heat is generated in the bulk. When the applied field reaches the peak, the derivative is null, the weld being at a higher temperature than the rest of the bulk, heat is transferred from the weld towards the bulk body. Then, when the applied field drops, heat is again generated in the bulk causing the weld temperature to increase again. Eventually, after the pulse, the weld heat is again transferred to the bulk body.

4. Discussion and conclusion

In this article, we have studied using FEM simulations the PFM of a REBaCuO comprising a superconducting weld with a self-field critical current density lower than the bulk body. We observed that during the pulse, the flux is entering the bulk through the weld and that a low J_c weld is easing the bulk magnetisation but reducing the maximum trapped field in complete penetration. However, for small values of applied field (<2 T), the overall trapped flux at the bulk surface is larger in the case of low J_c weld compared to a non-welded bulk. Additionally, for some values of applied fields, there is an optimal value of α leading to the maximum trapped flux. Therefore, the welding technique appears

to be uninteresting for very high field applications. Nevertheless, for low field applications, the superconducting welding technique may help to reach the higher trapped flux with a reduced applied field which is interesting in cases where the inductor coil size is limited such as electrical machines in where the bulks are to be magnetised from the armature and is not sized to generate very high field.

Moreover, the fast flux movement in the welding region is generating an important temperature rise. Hence, the thermal properties of the weld could be improved through doping in order to absorb or evacuate these losses more easily. The dopant could be included in the bulk in large quantities even at the expense of the weld critical current since the latter is to be smaller than the original material critical current. Thus, additional work is required to find the proper electromagnetic and thermal properties for the weld to maximise the trapped flux. Furthermore, the results presented in this paper need to be verified experimentally as many assumptions are made in the presented model.

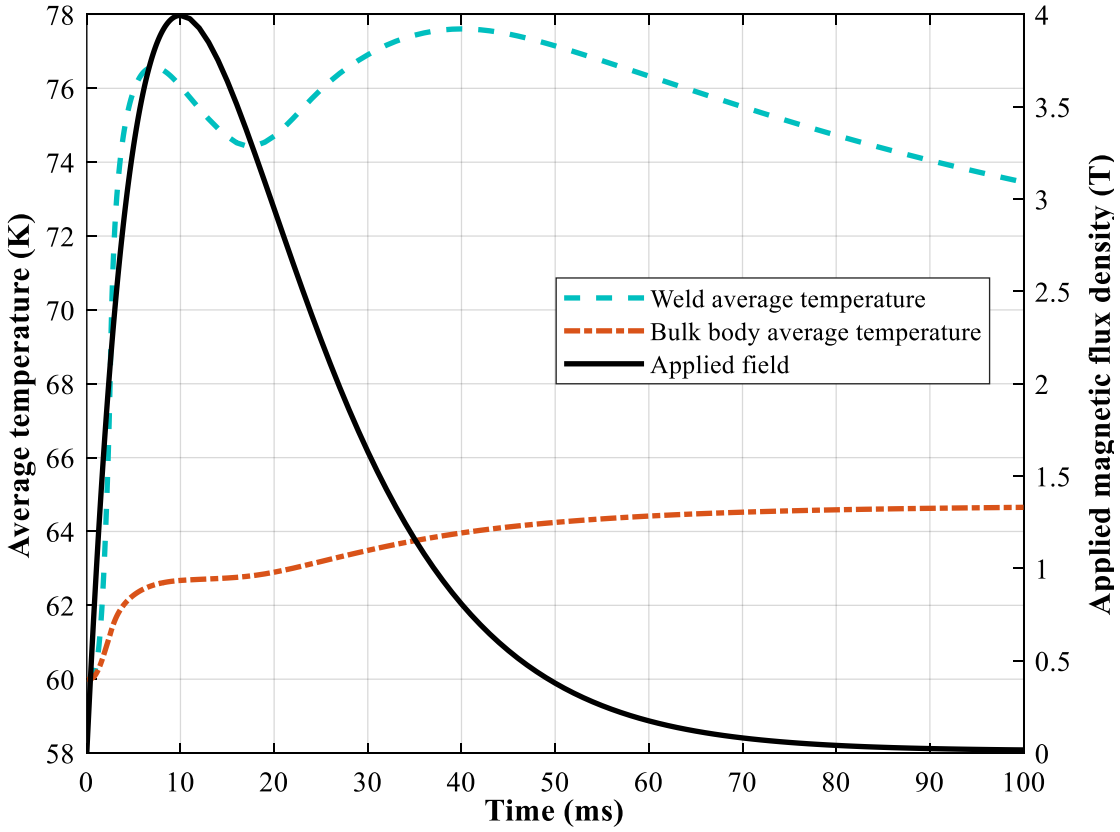

Figure 7. Left axis: Average temperature of the weld and the bulk body function of time during a 4 T pulse for $\alpha = 0.5$. Right axis: Applied magnetic flux density.

References

[1] Mukhopadhyay S M, Mahadev N and Sengupta S 2000 Microstructural and spectroscopic analyses of a strongly-linked joint formed in a superconductor *Physica C: Superconductivity* **329** 95–101

[2] Noudem J G, Reddy E S, Tarka M, Noe M and Schmitz G J 2001 Melt-texture joining of YBa2Cu3Oybulks *Supercond. Sci. Technol.* **14** 363–70

[3] Iida K, Yoshioka J, Sakai N and Murakami M 2002 Superconducting joint of Y–Ba–Cu–O superconductors using Er–Ba–Cu–O solder *Physica C: Superconductivity* **370** 53–8

[4] Iida K, Yoshioka J, Negichi T, Noto K, Sakai N and Murakami M 2002 Strong coupled joint for Y–Ba–Cu–O superconductors using a sintered Er–Ba–Cu–O solder *Physica C: Superconductivity* **378–381** 622–6

[5] Iida K, Yoshioka J, Sakai N and Murakami M 2003 Welding of different Y–Ba–Cu–O blocks *Physica C: Superconductivity* **392–396** 437–40

[6] Yoshioka J, Iida K, Negichi T, Sakai N, Noto K and Murakami M 2002 Joining Y123 bulk superconductors using Yb–Ba–Cu–O and Er–Ba–Cu–O solders *Supercond. Sci. Technol.* **15** 712–6

[7] Harnois C, Desgardin G, Laffez I, Chaud X and Bourgault D 2002 High quality weld of melt textured YBCO using Ag doped YBCO junctions *Physica C: Superconductivity* **383** 269–78

[8] Harnois C, Desgardin G and Chaud X 2001 A new way of welding YBa2Cu3O7-δ bulk textured domains *Supercond. Sci. Technol.* **14** 708–11

[9] Hopfinger T, Viznichenko R, Krabbes G, Fuchs G and Nenkov K 2003 Joining of multi-seeded YBCO melt-textured samples using YBCO/Ag composites as welding material *Physica C: Superconductivity* **398** 95–106

[10] Wei G, Guisheng Z, Xiao C, Aiping W, Jiarun H, Hailin B, Jialie R and Yulei J 2010 Joining of textured YBCO with YBCO added Ag2O additive *Physica C: Superconductivity* **470** 482–6

[11] Chai X, Zou G, Guo W, Wu A, He J, Bai H, Xiao L, Jiao Y and Jialie R 2010 Fast joining of melt textured Y–Ba–Cu–O bulks with high quality *Physica C: Superconductivity* **470** 598–601

[12] Yoshioka J, Iida K, Sakai N and Murakami M 2003 The crystallization in the welding region for Y–Ba–Cu–O bulk superconductors *Physica C: Superconductivity* **386** 495–9

[13] Harnois C, Chaud X, Laffez I and Desgardin G 2002 Joining of YBCO textured domains: a comparison between the multi-seeding and the welding techniques *Physica C: Superconductivity* **372–376** 1103–6

[14] Ainslie M D and Fujishiro H 2015 Modelling of bulk superconductor magnetization *Supercond. Sci. Technol.* **28** 053002

[15] Chen D -X. and Goldfarb R B 1989 Kim model for magnetization of type-II superconductors *Journal of Applied Physics* **66** 2489–500

[16] Berger K, Leveque J, Netter D, Douine B and Rezzoug A 2007 Influence of Temperature and/or Field Dependences of the $E-J$ Power Law on Trapped Magnetic Field in Bulk YBaCuO *IEEE Transactions on Applied Superconductivity* **17** 3028–31